International Symposium on Nonlinear Theory and its Applications
Xi'an, PRC, October 7–11, 2002

Auditory Evoked Fields (AEF) like Synthesized MEG Data Decomposition and Localization

Yoshio KONNO[1], Jianting CAO[2,3], Takayuki ARAI[1] and Andrzej CICHOCKI[3]

[1] Department of Electrical and Electronics Engineering, Sophia University
7-1 Kioicho, Chiyoda-ku, Tokyo, Japan
Phone: +81-3-3238-3411, Fax: +81-3-3238-3321, Email: [1]yy-konno@tc4.so-net.ne.jp
[2] Department of Electronics Engineering, Saitama Institute of Technology
1690 Fusaiji, Okabe, Saitama, Japan
Phone: +81-48-585-6854, Fax: +81-48-585-7030, Email: cao@sit.ac.jp
[3] Lab for Advanced Brain Signal Processing, BSI, RIKEN
2-1 Hirosawa, Wako-shi, Saitama, Japan

abstract In this paper, we apply an Independent Component Analysis (ICA) algorithm with pre-processing and post-processing techniques to decompose synthesized Magnetoencephalography (MEG) data. The behavior of our data set is similar to auditory evoked fields (AEFs). The main advantage for analyzing our synthesized data set is the location of evoked responses are known. The analyzed results are presented to illustrate the effectiveness and high performance both in source decomposition and source localization.

1. Introduction

A novel topic applying ICA to MEG data has been studied recently in order to determine the behavior and localization of brain sources [1]. During MEG signal detection, spontaneous and environmental noise may have considerable effect on recorded data, and therefore should be removed or considerably reduced. In this paper, we applied an additive noise reduction and optimizing dimensionality technique, Cao et al. developed [1]. In our procedure, for pre-processing, MEG data are first decomposed into uncorrelated signals with the reduction of additive noise and optimization of dimensionality. In the stage of source separation, decorrelated source signals are further decomposed into independent components by applying the joint approximate diagonalization of eigenmatrices (JADE) algorithm [2]. In the post-processing stage, we perform a source localization procedure to seek a single-EF map of decomposed individual components [1].

2. Method of data analysis

2.1. Time domain ICA

Based on the principle of MEG measurement, the problem can be formulated as

$$\mathbf{x}(t) = \mathbf{A}\mathbf{s}(t) + \mathbf{e}(t), \tag{1}$$

where $\mathbf{x}(t) = [x_1(t), \cdots, x_m(t)]^T$ represents the transpose of m observations at time t. Each observation $x_i(t)$ contains n common components (sources) $\mathbf{s}(t) = [s_1(t), \cdots, s_n(t)]^T$ and a unique component (additive noise) which is included in the vector $\mathbf{e}(t) = [e_1(t), \cdots, e_m(t)]^T$. $\mathbf{A} \in \mathbf{R}^{m\times n} = (a_{ij})$ can be represented by a numerical matrix whose element a_{ij} can be simply considered as a quantity related to the physical distance between the i-th sensor and the j-th source.

At first, we describe the robust pre-whitening technique [1], Cao et al. developed PCA algorithm with applying JADE to study high dimensional MEG data. The technique is very capable of reducing additive noise and optimizing dimensionality. In this technique, we can obtain the transform matrix as $\mathbf{Q} = [\hat{\mathbf{A}}^T \hat{\mathbf{\Psi}}^{-1} \hat{\mathbf{A}}]^{-1} \hat{\mathbf{A}}^T \hat{\mathbf{\Psi}}^{-1}$, where $\hat{\mathbf{A}}$ and $\hat{\mathbf{\Psi}}$ are estimates of $\mathbf{A}$ and $\mathbf{\Psi} = \mathbf{E}\mathbf{E}^T/N$ respectively. Using this transform matrix, a new data vector

$$\mathbf{z}(t) = \mathbf{Q}\mathbf{x}(t) \tag{2}$$

is obtained in which the power of noises, mutual correlation and dimensionality have been reduced. After pre-processing, the decomposed sources $\mathbf{y} \in \mathbf{R}^n$ can be obtained as

$$\mathbf{y}(t) = \mathbf{W}\mathbf{z}(t), \tag{3}$$

where $\mathbf{W} \in \mathbf{R}^{n\times n}$ is termed the demixing matrix which can be computed by using the JADE algorithm. JADE proposed in [2] can be used in the rotation procedure.

Next we describe the post-processing technique [1] to project the decomposed data onto the sensor space. Using $\hat{\mathbf{A}}$ and $\mathbf{W}$ with $\mathbf{y}$, we can obtain the virtual sensor

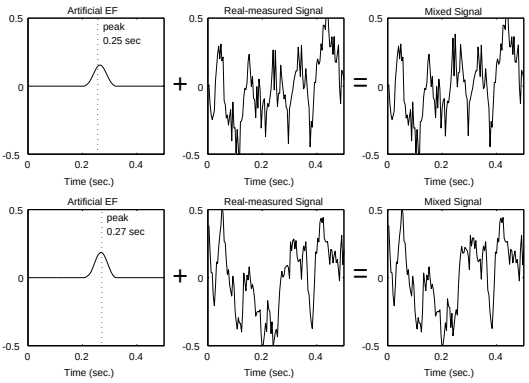

Figure 1: An example for data synthesization. (top) sensor-SL24 on trial1, (bottom) sensor-SL44 on trial1

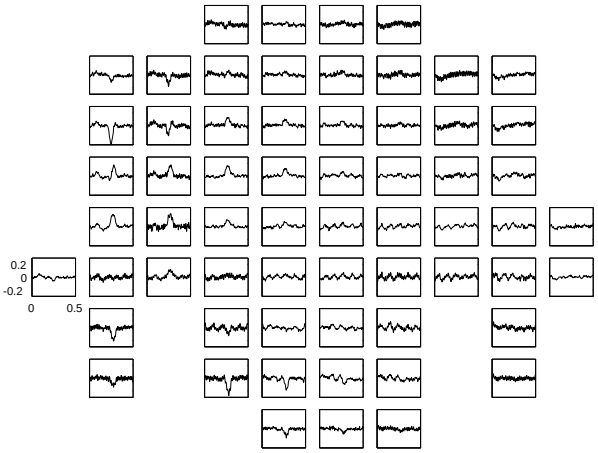

Figure 2: Result for averaged MEG data

signal contributed from multiple sources or an individual source as

$$\hat{\mathbf{x}}(t) = \hat{\mathbf{A}}\mathbf{W}^{-1}\mathbf{y}(t). \tag{4}$$

2.2. Frequency domain ICA

When signals are mixed in convolutive environments, the model can be described as

$$\mathbf{x}(t) = \mathbf{h} * \mathbf{s}(t) + \mathbf{e}(t) \tag{5}$$
$$\mathbf{z}(t) = \mathbf{Q} * \mathbf{x}(t) \tag{6}$$
$$\mathbf{y}(t) = \mathbf{W} * \mathbf{z}(t), \tag{7}$$

where $\mathbf{h} \in \mathbf{R}^{m \times n} = (h_{ij})$ is the impulse response from source j to sensor i and the $*$ is the convolution operator. Because it is possible to convert a convolution mixture in the time domain into an instantaneous mixture in the frequency domain, frequency domain BSS is effective for separating signals mixed in a reverberant environment.

Using a Fourier transform for (5-7), the model can be described as

$$\mathbf{X}(f) = \mathbf{H}\mathbf{S}(f) + \mathbf{E}(f) \tag{8}$$
$$\mathbf{Z}(f) = \mathbf{Q}\mathbf{X}(f) \tag{9}$$
$$\mathbf{Y}(f) = \mathbf{W}\mathbf{Z}(f), \tag{10}$$

where $\mathbf{X}(f) = [X_1(f), \cdots, X_m(f)]^T$ is the observed signal in the frequency domain, $\mathbf{Z}(t) = [Z_1(f), \cdots, Z_n(f)]^T$ are non correlative components by applying the robust pre-whitening technique and $\mathbf{Y}(f) = [Y_1(f), \cdots, Y_n(f)]^T$ is the estimated source signal by applying ICA.

3. Results for analyzing MEG data

3.1. AEFs like Synthesized MEG Data

In this subsection, we describe Auditory Evoked Fields (AEFs) like synthesized MEG data, used for simulation. The data is synthesized an artificial signal from two EFs (Fig. 1(left)) and the evoked-less MEG data (Fig. 1(middle)). The sampling frequency is 250 Hz, and observation trial time is 0.5 seconds per trial. Peak times at source signals are 0.25s for EF1 (Fig. 1(top)) and 0.27s for EF2 (Fig. 1(bottom)). The EF1 is located at $[x,\ y,\ z]_{s_1} = [10,\ 50,\ 50](mm)$ and The EF2 is located at $[x,\ y,\ z]_{s_2} = [-40,\ 40,\ 40](mm)$, where a head model presupposes a sphere with a radius of 75mm (see Fig. 4)). We take an average of 100 trials for data analysis, and we obtain an averaged data as shown in Fig. 2. Here the horizontal axis expresses time and the vertical axis expresses the output intensity of a sensor.

3.2. Results for Time domain ICA

3.2.1. Results for Data Decomposition

First we will demonstrate the source decorrelation applying time domain robust pre-whitening technique to the MEG data shown in Fig. 2. The results is shown in Fig. 3(a). In this simulation, the number of sources is assumed to be $n = 4$. Similar results were obtained for other conjectured numbers of sources. Using a 125-point short time Fourier transform for Fig. 3(a), we obtain these frequency contents shown in Fig. 3(b). Applying this technique, non correlative components are successfully extracted. z_1 has a peak time at 0.27s, so it's considered a source signal from EF2. z_2 has a high frequency at 50 Hz which may have been effected by electrical power interference. z_3 is a typical α-wave component of 10Hz. z_4 is considered a component mixed a source signal from EF1 and environment interference, which is incapable of being separated enough.

Although the robust pre-whitening technique can be used to reduce the additive noise and optimize dimen-

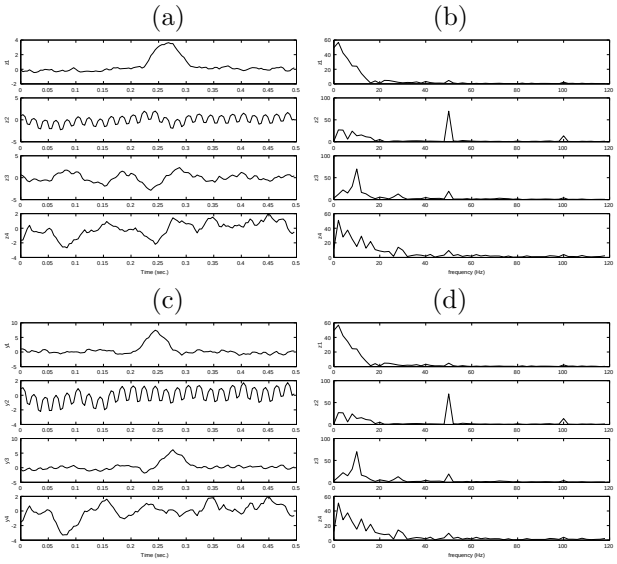

Figure 3: (a)Results for time domain pre-whitening, (b)Frequency contents of (a), (c)Results for time domain ICA, (d)Frequency contents of (c)

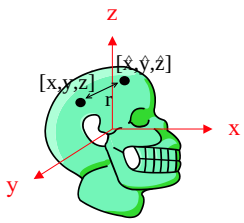

Figure 4: 3D visualization of EF location and the distance between the estimated EF and the true EF.

Table 1: The estimated EF location and the distance from true location applying time domain ICA [mm]

EF1	$\hat{x}$	$\hat{y}$	$\hat{z}$	r
averaged data	5.6	46.5	48.1	5.96
projecting y_1	10.8	47.7	50.9	2.56
projecting $y_1 + y_3$	7.7	45.8	50.8	4.84
EF2	$\hat{x}$	$\hat{y}$	$\hat{z}$	r
averaged data	-42.1	37.8	44.6	5.52
projecting y_3	-37.1	37.0	36.3	5.50
projecting $y_1 + y_3$	-43.4	36.6	41.7	5.17

sionality, it is insufficient to obtain independent sources, since some additional parameters must be further estimated. Applying time domain ICA to these new observations shown in Fig. 3(a), more clear signals have been extracted (Fig. 3(c)). Using a 125-point short time Fourier transform for Fig. 3(c), we obtain Fig. 3(d). y_3 and y_2 are practically considered z_1 and z_2 respectively. y_1 has a peak time at 0.25s, so it's considered a source signal from EF1. z_4 is considered environment interference, whose power is reduced by the taking average.

This result illustrates that the estimate $\hat{\mathbf{A}}\mathbf{W}^{-1}$ obtained by using ICA with the robust pre-whitening techniques approximates the true matrix $\mathbf{A}$ more accurately than the estimate $\hat{\mathbf{A}}$ obtained by using only the pre-whitening technique.

3.2.2. Results for Data Localization

In this subsection, we first demonstrate the source Localization described in Section 2. We applied the source localization to 3 types of decomposed data (y_1, y_3, $y_1 + y_3$), projecting those decomposed signals onto the sensor space using Eq. (4).

Next we applied the standard spatio-temporal dipole fitting routine to the pre-analyzed MEG signal and those virtually measured signals. Applying this routine, we can obtain estimated EFs locations. Furthermore using the next equation about the distance between true EF locations $[x,\ y,\ z]$ and estimated EF locations $[\hat{x},\ \hat{y},\ \hat{z}]$ as

$$r = \sqrt{(x-\hat{x})^2 + (y-\hat{y})^2 + (z-\hat{z})^2}, \qquad (11)$$

we can compare the results derived by the propose method with the pre-analyzed data. Here $[x,\ y,\ z]_{s_1} = [10,\ 50,\ 50]$ and $[x,\ y,\ z]_{s_2} = [-40,\ 40,\ 40]$ (see Fig. 4).

First we will demonstrate the results about EF1. The estimated EF location at the pre-analyzed data is $[\hat{x},\ \hat{y},\ \hat{z}]^{ave}_{\hat{s_1}} = [5.6,\ 46.5,\ 48.1]$, so the distance from true EF location has become $r^{ave}_{\hat{s_1}} = 5.96$ mm. On the other hand, at the virtually measured signal projected the decomposed signal y_1, the estimated EF location is $[\hat{x},\ \hat{y},\ \hat{z}]^{y_1}_{\hat{s_1}} = [10.8,\ 47.7,\ 50.9]$, and the distance has become $r^{y_1}_{\hat{s_1}} = 2.56$ mm (smaller than $r^{ave}_{\hat{s_1}}$). At the virtually measured signal projected decomposed signals $y_1 + y_3$, the estimated EF location is $[\hat{x},\ \hat{y},\ \hat{z}]^{y_1+y_3}_{\hat{s_1}} = [7.7,\ 45.8,\ 50.8]$, and the distance has become $r^{y_1+y_3}_{\hat{s_1}} = 4.84$ mm (Tab. 1).

Next we demonstrate results about EF2. The estimated EF location at the pre-analyzed data is $[\hat{x},\ \hat{y},\ \hat{z}]^{ave}_{\hat{s_2}} = [-42.1,\ 37.8,\ 44.6]$, so the distance from true EF location ($[x,\ y,\ z]_{DP2} = [-40,\ 40,\ 40]$) has become $r^{ave}_{\hat{s_2}} = 5.52$ mm. On the other hand, at the virtually measured signal projected the decomposed signal y_3, the estimated EF location is $[\hat{x},\ \hat{y},\ \hat{z}]^{y_3}_{\hat{s_2}} = [-37.1,\ 37.0,\ 36.3]$, and the distance has become $r^{y_3}_{\hat{s_2}} = 5.50$ mm. At the virtually measured signal projected decomposed signals $y_1 + y_3$, the estimated EF location is $[\hat{x},\ \hat{y},\ \hat{z}]^{y_1+y_3}_{\hat{s_2}} = [-43.4,\ 36.6,\ 41.7]$, and the distance has become $r^{y_1+y_3}_{\hat{s_2}} = 5.17$ mm (see Tab. 1).

Comparing the results derived by the proposed method with the results for pre-analyzed data, we can conclude that the proposed algorithms work very efficiently, and the performance is better than that of the pre-analyzed results.

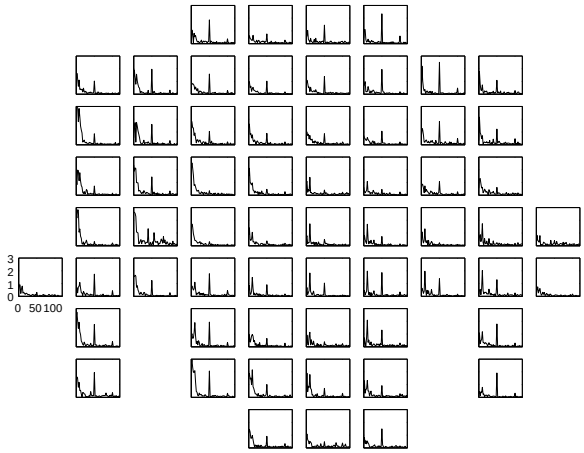

Figure 5: Frequency contents of averaged MEG data

3.3. Results for Frequency domain ICA

3.3.1. Results for Data Decomposition

In this subsection, we demonstrate the source decompositions by frequency domain robust pre-whitening technique and frequency domain ICA. At first, applying a 125-point short time Fourier transform to the averaged MEG data shown in Fig. 2, we obtain the frequency contents of the averaged MEG data shown in Fig. 5. The results of pre-whitening and ICA are shown in Fig. 6(a) and (c) respectively. Using a 125-point Inverse Fourier transform for Fig. 5(a) and (c), we obtain these time contents as shown in Fig. 6(b) and (d).

The results of frequency domain pre-whitening practically correspond with the results for time domain pre-whitening. At the results for ICA, y_1 has a peak time at 0.25-0.27 ms, so it's considered the component mixed a source signal from EF1 and a source signal from EF2. y_2 is a signal effected by electrical power interference at 50 Hz. y_3 has a frequency at 10 Hz, so it's considered a typical α-wave content. z_4 is considered environment interference, its power is reduced by taking its average.

3.3.2. Results for Data Localization

We applied the source localization to the decomposed data y_1, projecting this decomposed signal onto the sensor space using Eq. (4). Next we applied the standard spatio-temporal dipole fitting routine to the virtually measured signals (see Tab. 2). Let us first demonstrate the result about EF1. The estimated EF location at the virtually measured signal projected the decomposed signal y_1 is $[\hat{x},\ \hat{y},\ \hat{z}]^{y_1}_{\hat{s_1}} = [10.1,\ 53.4,\ 51.24]$, and the distance from true EF1 location has become $r^{y_1}_{\hat{s_1}} = 3.65$ mm . About EF2, the estimated location is $[\hat{x},\ \hat{y},\ \hat{z}]^{y_1}_{\hat{s_2}} = [-40.9,\ 41.25,\ 40.44]$, and the distance has become $r^{y_1}_{\hat{s_2}} = 1.61$ mm (see Tab. 2).

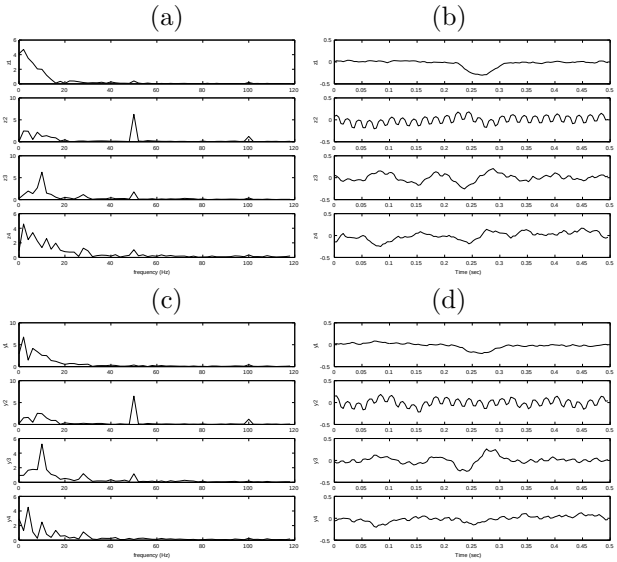

Figure 6: (a)Results for frequency domain pre-whitening, (b)Time domain contents of (a), (c)Results for frequency domain ICA, (d)Time domain contents of (c)

Table 2: The estimated EF location and the distance from true location applying frequency domain ICA [mm]

	$\hat{x}$	$\hat{y}$	$\hat{z}$	r
EF1	10.12	53.43	51.24	3.65
EF2	-40.91	41.25	40.44	1.61

Comparing the results for time domain ICA with the results for frequency domain ICA, Time domain ICA is more effective at data decomposition. At data localization, in contrast, Frequency domain ICA is more effective.

4. Conclusions

In this paper, we analyzed AEF like synthesized MEG data applying proposed method. The analyzed results are presented to illustrate the effectiveness and high performance both in source decomposition and source localization. In further works, we will develop the ICA algorithm for not averaged single-trial data analysis.

References

[1] J. Cao, N. Murata, S. Amari, A. Cichocki and T. Takeda: A Robust Approach to Independent Component Analysis of Signals with High-Level Noise Measurements, IEEE Trans. on Neural Networks (in print).

[2] J. F. Cardoso and A. Souloumiac: Jacobi angles for simultaneous diagonalization, SIAM J. Mat. Anal. Appl., Vol. 17, No. 1, pp. 145-151, 1996.